

Crossover behavior from decoupled criticality

Y. Kamiya,¹ N. Kawashima,¹ and C. D. Batista²

¹*Institute for Solid State Physics, University of Tokyo, Kashiwa, Chiba 227-8581, Japan*

²*Theoretical Division, Los Alamos National Laboratory, Los Alamos, New Mexico 87545, USA*

(Received 26 July 2010; published 24 August 2010)

We study the thermodynamic phase transition of a spin Hamiltonian comprising two three-dimensional (3D) magnetic sublattices. Each sublattice contains XY spins coupled by the usual bilinear exchange while spins in different sublattices only interact via biquadratic exchange. This Hamiltonian is an effective model for XY magnets on certain frustrated lattices such as body centered tetragonal. By performing a cluster Monte Carlo simulation, we investigate the crossover from the 3D-XY fixed point (decoupled sublattices) and find a systematic flow toward a first-order transition without a separatrix or a new fixed point. This strongly suggests that the correct asymptotic behavior is a first-order transition.

DOI: [10.1103/PhysRevB.82.054426](https://doi.org/10.1103/PhysRevB.82.054426)

PACS number(s): 05.70.Jk, 05.50.+q, 75.30.Kz, 75.40.Mg

I. INTRODUCTION

Geometric frustration can play a decisive role in the behavior of magnetic systems. The combination of frustrated geometries with strong quantum fluctuations can lead to new quantum states of matter.¹⁻³ It has been shown recently that novel charge effects in Mott insulators, such as spin-driven electronic charge-density waves, or orbital currents, only take place in geometrically frustrated lattices.⁴ Geometric frustration can also reduce the effective dimensionality of certain quantum critical points.⁵ Finally, it has been known for years that the presence of geometric frustration can change the nature of certain thermodynamic phase transitions. However, it has been also recognized that the nature of the new transition can be very elusive for the standard renormalization-group treatments⁶ and may require very sophisticated numerical approaches.^{7,8}

Several quantum magnets comprise two sublattices of magnetic ions coupled by a geometrically frustrated exchange.⁵ This is for instance the case of a Heisenberg antiferromagnet on a body centered tetragonal (BCT) lattice⁹ or a square lattice with nearest- and next-nearest-neighbor exchange interactions.^{10,11} We are interested in the regime of intersublattice coupling smaller than the intrasublattice exchange. We will also assume that there is a uniaxial easy-plane anisotropy that reduces the Hamiltonian symmetry from O(3) to O(2). The frustrated nature of the intersublattice exchange precludes a bilinear coupling between the order parameters of the two sublattices. The Hamiltonian symmetry only allows for an effective *biquadratic* coupling. Consequently, if \mathbf{m}_A and \mathbf{m}_B are the XY magnetizations at wave vector $\mathbf{k}_0=(\pi, \pi, 0)$ of the sublattices (which in the BCT lattice case are the even- and odd-numbered layers⁹), the parallel or antiparallel orientations of \mathbf{m}_A and \mathbf{m}_B correspond to different ground states. The Z_2 symmetry is broken by selecting one of these two states.^{9,12-14} The O(2) \times Z_2 symmetry breaking also appears in the XY model on a triangular lattice.¹⁵ In this case the Z_2 broken symmetry corresponds to the two possible vector chiral orderings.

We want to explore the nature of the thermodynamic phase transition associated with the O(2) \times Z_2 symmetry breaking that takes place in several frustrated magnets. For

this purpose, we will consider classical magnetic moments because the quantum character of the spins does not affect the nature of the thermodynamic transition. In Ref. 9, we used two different approaches to understand the effect of the additional Z_2 symmetry breaking and compared their results. The first approach was a Monte Carlo (MC) simulation of the classical spin model on the BCT lattice. The second approach was a scaling analysis of the Landau-Ginzburg-Wilson (LGW) model that preserves the symmetries of the lattice Hamiltonian. A single transition with exponents close to those of the 3D XY model was obtained from a finite-size scaling (FSS) analysis of the MC data.⁹ On the other hand, the scaling analysis of the LGW model

$$H_{\text{LGW}} = \int d^d x \left[\sum_{a=A,B} \left(\frac{1}{2} |\nabla \phi_a|^2 + t |\phi_a|^2 + u |\phi_a|^4 \right) + \lambda (\phi_A \cdot \phi_B)^2 + g |\phi_A|^2 |\phi_B|^2 \right] \quad (1)$$

indicated that λ is a relevant perturbation for the 3D XY decoupled fixed point (DFP) located on the u axis ($u \neq 0$, $\lambda = g = 0$).⁹ Here, $\phi_a = (\phi_a^x, \phi_a^y)$ ($a=A, B$) is a two-component field representing antiferromagnetic moments in even- ($a=A$) or odd- ($a=B$) numbered layers, and λ is the biquadratic coupling between them. These results look contradicting at a first glance: although the numerical observations can be explained in a consistent way by the DFP, this fixed point is nevertheless *unstable* along the λ direction. More specifically, near the DFP, λ transforms as $\lambda' = b^{y_\lambda} \lambda$, where $y_\lambda = 0.526(8)$ and b is a rescaling factor.⁹

The scaling argument implies that there will be a crossover behavior from the DFP, provided $|\lambda|L^{y_\lambda} \gtrsim 1$ with L being the system size.⁹ However, $|\lambda|$ can be quite small for the original frustrated spin system because it is an effective interaction that arises from second-order perturbation with respect to the ratio between the interlayer and the intralayer bilinear exchange couplings.⁹ In addition, we could not obtain data for sufficiently large L in our previous calculation in Ref. 9 because we simulated the original Hamiltonian on the *frustrated* lattice. Thus, the nature of the crossover was left as an open problem.

II. MODEL AND METHOD

A. Model

In this paper, we explore the expected crossover by studying an XY spin model on a cubic lattice that is more directly related to the LGW effective model than to the original Hamiltonian on the BCT lattice. The relevant coupling λ is explicitly taken into account by considering the Hamiltonian model

$$H = -J \sum_{\langle i,j \rangle, a=A,B} \mathbf{S}_{a,i} \cdot \mathbf{S}_{a,j} + \lambda J \sum_i (\mathbf{S}_{A,i} \cdot \mathbf{S}_{B,i})^2 \quad (2)$$

with $J > 0$. $\mathbf{S}_{a,i}$ ($a=A, B$) is a classical XY spin at site i on the cubic lattice and $\langle i, j \rangle$ is a pair of nearest-neighbor sites. The coefficient λ characterizes the amplitude of the biquadratic coupling that is expected to drive the system away from the DFP. We consider the case $\lambda < 0$, which is experimentally relevant.⁹ No term corresponding to the g term in H_{LGW} is explicitly included in H because it is automatically generated when the short wavelength modes are integrated out (renormalization process).

In the ground state, both A and B spins are ferromagnetically ordered and the $O(2)$ symmetry is broken. In addition, their relative phase is locked so that $\mathbf{S}_{A,i} \cdot \mathbf{S}_{B,i} = \pm 1$, which causes Z_2 symmetry breaking. The order parameters associated with these two kinds of symmetry breaking are $\mathbf{m} = \mathbf{m}_A$ with $\mathbf{m}_A = L^{-d} \sum_i \mathbf{S}_{a,i}$ and $\sigma = L^{-d} \sum_i \sigma_i$ with $\sigma_i = \mathbf{S}_{A,i} \cdot \mathbf{S}_{B,i}$, respectively. We introduce the correlation functions $G_{ij}^m = \langle \mathbf{S}_{A,i} \cdot \mathbf{S}_{A,j} \rangle$ and $G_{ij}^\sigma = \langle \sigma_i \sigma_j \rangle$. (For the definition of \mathbf{m} and G_{ij}^m , we can use either A or B spins without loss of generality.)

For very small $|\lambda|$ ($\lambda = -0.05$, $L \leq 64$), we observe an apparently continuous transition with exponents of the DFP, which is naturally interpreted as the same behavior as in the previous MC simulation in Ref. 9. However, a more careful FSS analysis reveals the expected crossover. We present a numerically obtained renormalization-group flow diagram of several scaling parameters that should be scale invariant at the second-order transitions.^{7,8} We find that the flow evolves systematically from the DFP without a sign of a stable fixed point or a separatrix, toward the region where the transition is discontinuous. Based on this observation and the lack of a stable fixed point in the ϵ expansion ($\epsilon = 4 - d$) around the DFP,¹⁶ we propose that the correct asymptotic behavior is a first-order transition for any (negative) finite value of λ .

B. Method

The absence of explicit frustration is the main computational advantage of H relative to the original model studied in Ref. 9. This enables us to develop an efficient cluster MC algorithm based on a minor modification of the embedding method proposed by Wolff.¹⁷ In every update cycle, we choose a unit vector \mathbf{n} at random. The vector \mathbf{n} defines the Z_2 transformations $\bar{\mathbf{S}}_A = \mathbf{S}_A - 2(\mathbf{S}_A \cdot \mathbf{n})\mathbf{n}$ and $\bar{\mathbf{S}}_B = -\mathbf{S}_B + 2(\mathbf{S}_B \cdot \mathbf{n})\mathbf{n}$. (The difference by a factor of -1 serves to enhance the relaxation of the σ modes as compared to applying the same mirror-image transformation to the A and B spins.) Then, we choose a spin $\mathbf{S}_{a,i}$ and identify a cluster $C = \{\mathbf{S}_{a,i}, \mathbf{S}_{b,j}, \mathbf{S}_{c,k}, \dots\}$ that can be reached from $\mathbf{S}_{a,i}$ via proba-

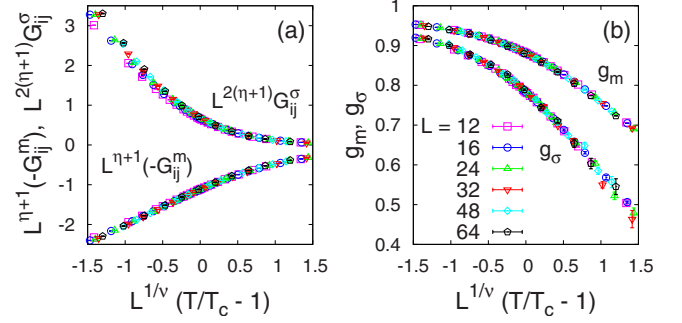


FIG. 1. (Color online) Pseudoscaling behavior observed for $\lambda = -0.05$ ($|\lambda|L^{2\nu} \approx 0.45$ for $L=64$) of (a) correlation functions at a distance $r_{ij,x}=r_{ij,y}=r_{ij,z}=L/2$ and (b) correlation ratios. Here, η and ν are critical exponents of the 3D XY model. $T_c/J \approx 2.2021$ is obtained from the crossings of dimensionless scaling parameters.

bilistically activated links. The probability to activate a link depends on the interaction on the link: $P_1(\mathbf{S}, \mathbf{S}') = 1 - \min\{1, \exp[\beta J(\bar{\mathbf{S}} - \mathbf{S}) \cdot \mathbf{S}']\}$ for links with the bilinear exchange and $P_2(\mathbf{S}, \mathbf{S}') = 1 - \min(1, \exp\{|\lambda| \beta J [(\bar{\mathbf{S}} \cdot \mathbf{S}')^2 - (\mathbf{S} \cdot \mathbf{S}')^2])\}$ for links with the biquadratic coupling. After a cluster is identified, we flip it, namely, apply the Z_2 transformation on every spin included in C . It can be easily checked that the algorithm satisfies both the detailed-balance and ergodicity conditions.

III. RESULTS

A. Conventional scaling analysis

We first present the results for very small $|\lambda|$ with $|\lambda|L^{2\nu} \lesssim 1$, where we observe an apparently continuous transition controlled by the DFP. This is naturally expected from the scaling argument given above and basically the same behavior that was observed in the frustrated model previously studied in Ref. 9. In Fig. 1(a), we present the FSS plots of G_{ij}^m and G_{ij}^σ at the largest distance in a given system, where $r_{ij,x}=r_{ij,y}=r_{ij,z}=L/2$ ($\lambda = -0.05$, $L \leq 64$). These plots are based on the following FSS forms at the DFP:⁹ $G_{ij}^m(T, L, r_{ij}) \sim L^{-(\eta+1)} f_m[L^{1/\nu}(T-T_c), r_{ij}/L]$ and $G_{ij}^\sigma(T, L, r_{ij}) \sim L^{-2(\eta+1)} f_\sigma[L^{1/\nu}(T-T_c), r_{ij}/L]$ with $\eta = 0.0380(4)$ and $\nu = 0.68155(27)$ being the critical exponents of the 3D XY model.¹⁸ Using the exponent of the DFP, we can also produce reasonable FSS plots for the correlation ratios g_m and g_σ ,¹⁹ defined by ratios of the corresponding correlation functions at two different distances $r_{ij,x}=r_{ij,y}=r_{ij,z}=L/2, L/4$ [see Fig. 1(b)].

However, since the scaling argument shows that the DFP is unstable, we conclude that these FSS plots simply describe the “pseudoscaling” behavior, i.e., as long as $|\lambda|$ is finite, significant deviations should eventually appear in large enough lattices. In other words, we cannot conclude that the transition is of second order because weak first-order transitions can become practically indistinguishable from continuous transitions in the usual FSS analysis for small L . Indeed, for relatively large $|\lambda|$, we find obvious deviations from the DFP. As shown in Figs. 2(a) and 2(b), the energy distributions near the transition show a bimodal structure with in-

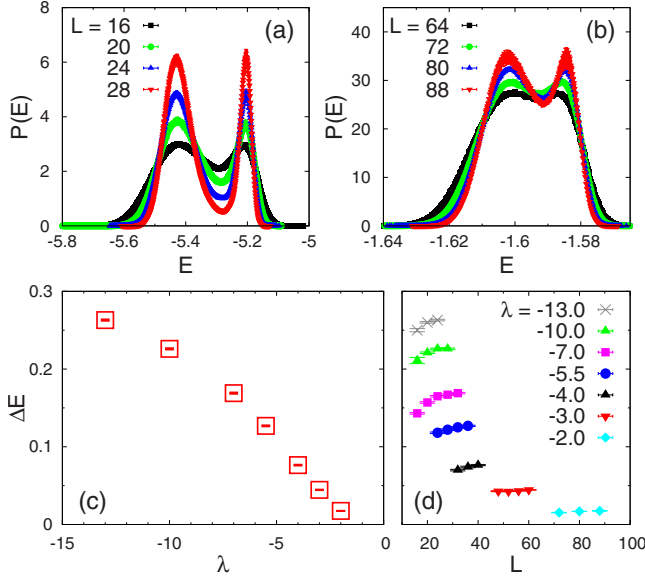


FIG. 2. (Color online) Bimodal energy distribution at $T \approx T_c$ for (a) $\lambda = -10$ ($|\lambda|L^{y_\lambda} \approx 43$ for $L=16$) and (b) $\lambda = -2$ ($|\lambda|L^{y_\lambda} \approx 18$ for $L=64$). Most error bars are smaller than the symbol sizes. (c) Peak-to-peak distance of the distribution corresponding to the latent heat for the largest L for each λ . (d) System-size dependence of the peak-to-peak distance.

creasing depth for larger system sizes. This is clear evidence for a first-order transition. The peak-to-peak distance gives an estimate of the latent heat $\Delta E(\lambda)$. As expected, the first-order nature becomes weaker for smaller $|\lambda|$ [see Fig. 2(c)].

B. Monte Carlo renormalization-group analysis

Given our results for small and large values of $|\lambda|$, it is natural to ask if there is a multicritical point where the first-order transition line terminates. The dependence of $\Delta E(\lambda)$ on small values of $|\lambda|$ does not provide an efficient way of answering this question because larger lattices are required to detect smaller values of ΔE . In what follows, we explain our method to investigate the correct asymptotic behavior for very small $|\lambda|$. Our approach is a sort of MC renormalization-group analysis.^{7,8} A similar technique was applied, for instance, to the random-bond Ising model by Hukushima and it was found that the method is very useful to obtain qualitative structure of the phase diagram.⁷

We consider several dimensionless scaling parameters $R(\lambda)$ (such as g_m and g_σ defined above) and introduce their L -dependent estimators $R(\lambda, L)$ as the crossings of temperature-dependent curves of the parameters for two successive system sizes L and $2L$. Because the $L \rightarrow \infty$ limit, $R(\lambda)$, is expected to be scale invariant and universal for a second-order transition, $R(\lambda, L)$ must converge to such a universal value if the transition is continuous. Consequently, if a multicritical point exists, the “flow” structure of $R(\lambda, L)$ should have a separatrix and a stable fixed point. Here, the term flow refers to the evolution of $R(\lambda, L)$ with increasing L .

In addition to g_m and g_σ , we use as $R(\lambda, L)$ the Binder parameters defined by $U_m = \langle |\mathbf{m}|^4 \rangle / \langle |\mathbf{m}|^2 \rangle^2$ and $U_\sigma =$

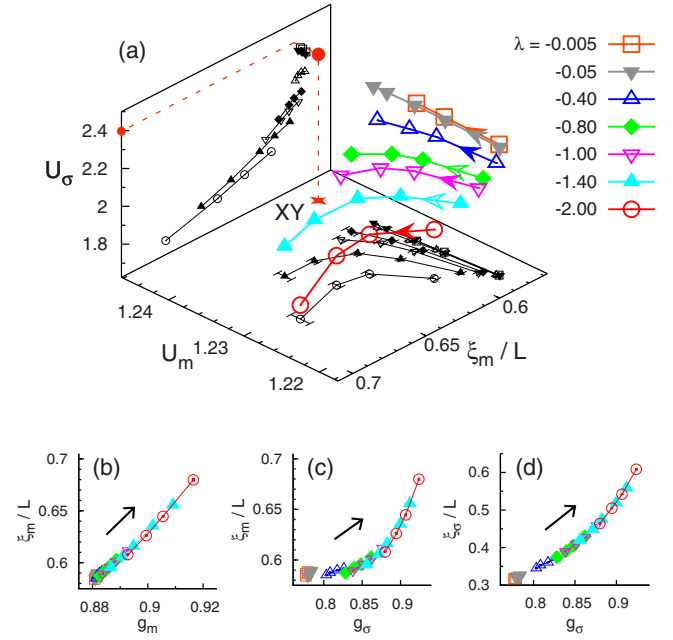


FIG. 3. (Color online) (a) The flow diagram projected onto the $(U_m, \xi_m/L, U_\sigma)$ space. Two-dimensional projections are also shown. Error bars for U_m are shown on the bottom plane and those for the other parameters are smaller than the symbol size (not shown). System sizes corresponding to the data points in each flow are $L = 8, 12, 16, 24$ (not for $\lambda = -0.005$) and 32 (only for $\lambda = -0.05, -1.4$), in order specified by arrows attached to the flow lines. The DFP projected on the $(U_m, \xi_m/L)$ plane is denoted by “XY.” $U_\sigma \approx 2.40(1)$ at the DFP is estimated by extrapolating the $\lambda = -0.005$ flow and it is shown by a small filled circle on the U_σ axis. [(b)–(d)] The same flow diagrams projected on the other subspaces. The arrows show the overall direction of the flows.

$= \langle \sigma^4 \rangle / \langle \sigma^2 \rangle^2$, and the second-moment correlation lengths²⁰ divided by the system size ξ_m/L and ξ_σ/L . Hence, the entire parameter space is six-dimensional in our treatment. The obtained flow diagrams are shown in Fig. 3. As can be seen in Figs. 3(b)–3(d), we find that in the four-dimensional subspace $(g_m, \xi_m/L, g_\sigma, \xi_\sigma/L)$ trajectories of the projected flows collapse on an approximately single, monotonous curve. Therefore, it turns out to be sufficient to treat the projected flow in the subspace spanned by one of the above four (we choose ξ_m/L) and the other two parameters not included here, namely U_m and U_σ .

The flow projected onto this $(U_m, \xi_m/L, U_\sigma)$ subspace is shown in Fig. 3(a). The DFP is associated with the flows for $\lambda = -0.005$ or -0.05 , because, as is implied by the data collapse in the FSS plots shown in Fig. 1, with such small $|\lambda|$ the effect of the biquadratic perturbation is still negligible in the length scale under consideration. The known estimates for the 3D XY universality class are $U_m = 1.2430(5)$ and $\xi_\sigma/L = 0.5925(2)$.¹⁸ We show the point corresponding to these values on the $(U_m, \xi_m/L)$ plane in Fig. 3(a). (Estimates for the other less common parameters are not available in the literature as far as we know.) The above observation is in good agreement with these estimates.

For larger values of $|\lambda|$ with $|\lambda|L^{y_\lambda} \geq 1$, the flow clearly deviates from the trajectory dominated by the DFP. This is a

clear sign of the expected crossover. The crossover is already evident for $\lambda = -0.4$ ($|\lambda|L^{y_\lambda} \approx 3.1$ for $L=48$). As $|\lambda|$ increases, the flow keeps evolving away from the DFP without a stable fixed point or a separatrix. Note that we have already shown clear evidence of a first-order transition for $\lambda = -2$ [Fig. 2(b)]. This indicates that the observed crossover eventually leads to the first-order transition.

While the numerical evidence in finite systems is always insufficient for very small $|\lambda|$, we take the numerical result presented above as a strong evidence for the first-order character of arbitrary small $|\lambda|$. This conclusion is also supported by the epsilon expansion analysis of H_{LGW} around the DFP:¹⁶ the result obtained by expanding the Hamiltonian to $O(\epsilon)$ is most naturally explained as the lack of a separatrix fixed point, suggesting a fluctuation-induced first-order transition.

IV. SUMMARY

To summarize, we have established the crossover behavior from the 3D XY DFP for an effective model that is relevant for several frustrated magnets near their thermodynamic phase transitions. Such crossover results in a weakly first-order phase transition. Our calculation also shows that it will be very difficult to observe such a first-order transition with standard experimental methods as long as the frustrated interlayer coupling is small in comparison with the intralayer exchange. This is indeed the case of $\text{BaCuSi}_2\text{O}_6$ (Ref. 21) as discussed in Ref. 9. In other words, although the correct asymptotic behavior is the first-order transition, the thermodynamic behavior will be dominated by the 3D XY DFP in a broad region near the transition. The true discontinuous nature of the transition can be observed in a very narrow region near the transition point that could easily be beyond the ex-

perimental precision in most cases. Nevertheless, the first-order transition should be observable for frustrated magnets with $|\lambda|$ of order one. In such cases, the 3D XY-like behavior beyond a certain distance from the transition point will be finally interrupted by the fluctuation-induced first-order transition.

A value of $|\lambda|$ of order 1 is indeed realized in the frustrated spin model that has been proposed for describing the iron based superconductors $\text{LaFeAs}(\text{O}_{1-x}\text{F}_x)$.^{22,23} According to our result, such a model should exhibit a single weakly first-order transition to the broken $\text{O}(2) \times \text{Z}_2$ phase in presence of a strong magnetic field [the field is required to induce effective $\text{O}(2)$ magnetic moments]. The stacked triangular antiferromagnetic compounds²⁴ are other physical realizations of the effective model considered here [Eq. (2)]. Similarly, we predict a single weakly first-order phase transition to take place in these systems in presence of a strong magnetic field, which is in agreement with recent investigations.^{8,25}

ACKNOWLEDGMENTS

We would like to thank M. Oshikawa and Y. Tomita for illuminating suggestions. The computation in the present work is executed on computers at the Supercomputer Center, Institute for Solid State Physics, University of Tokyo, and T2K Open Supercomputer, University of Tokyo. The project is supported by the MEXT Global COE Program “the Physical Science Frontier,” the MEXT Grand-in-Aid for Scientific Research (B) (Grant No. 22340111), the MEXT Grand-in-Aid for Scientific Research on Priority Areas “Novel States of Matter Induced by Frustration” (Grant No. 19052004), and by the Next Generation Supercomputing Project, Nanoscience Program, MEXT, Japan.

-
- ¹H. Kageyama, K. Yoshimura, R. Stern, N. V. Mushnikov, K. Onizuka, M. Kato, K. Kosuge, C. P. Slichter, T. Goto, and Y. Ueda, *Phys. Rev. Lett.* **82**, 3168 (1999).
- ²K. Kodama, M. Takigawa, M. Horvatic, C. Berthier, H. Kageyama, Y. Ueda, S. Miyahara, F. Becca, and F. Mila, *Science* **298**, 395 (2002).
- ³S. E. Sebastian, N. Harrison, P. Sengupta, C. D. Batista, S. Francoual, E. Palm, T. Murphy, N. Marcano, H. A. Dabkowska, and B. D. Gaulin, *Proc. Natl. Acad. Sci. U.S.A.* **105**, 20157 (2008).
- ⁴L. N. Bulaevskii, C. D. Batista, M. V. Mostovoy, and D. I. Khomskii, *Phys. Rev. B* **78**, 024402 (2008).
- ⁵S. E. Sebastian, N. Harrison, C. D. Batista, L. Balicas, M. Jaime, P. A. Sharma, N. Kawashima, and I. R. Fisher, *Nature (London)* **441**, 617 (2006).
- ⁶B. Delamotte, Y. Holovatch, D. Ivaneyko, D. Mouhanna, and M. Tissier, *J. Stat. Mech.: Theory Exp.* (2008) P03014.
- ⁷K. Hukushima, *J. Phys. Soc. Jpn.* **69**, 631 (2000).
- ⁸M. Itakura, *J. Phys. Soc. Jpn.* **72**, 74 (2003).
- ⁹Y. Kamiya, N. Kawashima, and C. D. Batista, *J. Phys. Soc. Jpn.* **78**, 094008 (2009).
- ¹⁰C. L. Henley, *Phys. Rev. Lett.* **62**, 2056 (1989).
- ¹¹P. Chandra, P. Coleman, and A. I. Larkin, *Phys. Rev. Lett.* **64**, 88 (1990).
- ¹²C. D. Batista, J. Schmalian, N. Kawashima, P. Sengupta, S. E. Sebastian, N. Harrison, M. Jaime, and I. R. Fisher, *Phys. Rev. Lett.* **98**, 257201 (2007).
- ¹³O. Rösch and M. Vojta, *Phys. Rev. B* **76**, 180401(R) (2007).
- ¹⁴J. Schmalian and C. D. Batista, *Phys. Rev. B* **77**, 094406 (2008).
- ¹⁵M. Hasenbusch, A. Pelissetto, and E. Vicari, *J. Stat. Mech.: Theory Exp.* (2005) P12002.
- ¹⁶A. Aharony, *Phys. Rev. B* **12**, 1038 (1975).
- ¹⁷U. Wolff, *Phys. Rev. Lett.* **62**, 361 (1989).
- ¹⁸M. Campostrini, M. Hasenbusch, A. Pelissetto, P. Rossi, and E. Vicari, *Phys. Rev. B* **63**, 214503 (2001).
- ¹⁹Y. Tomita and Y. Okabe, *Phys. Rev. B* **66**, 180401(R) (2002).
- ²⁰F. Cooper, B. Freedman, and D. Preston, *Nucl. Phys. B* **210**, 210 (1982).
- ²¹Ch. Rüegg, D. F. McMorrow, B. Normand, H. M. Rønnow, S. E. Sebastian, I. R. Fisher, C. D. Batista, S. N. Gvasaliya, Ch. Niedermayer, and J. Stahn, *Phys. Rev. Lett.* **98**, 017202 (2007).
- ²²C. Xu, M. Müller, and S. Sachdev, *Phys. Rev. B* **78**, 020501(R) (2008).
- ²³C. Fang, H. Yao, W.-F. Tsai, J. P. Hu, and S. A. Kivelson, *Phys. Rev. B* **77**, 224509 (2008).
- ²⁴H. Kawamura, *J. Phys.: Condens. Matter* **10**, 4707 (1998).
- ²⁵V. Ngo and H. Diep, *J. Appl. Phys.* **103**, 07C712 (2008).